Concentration- and Density-Fluctuations with Amorphous $Ni_{63}Nb_{37}$ by Means of Neutron Scattering at Small Momentum Transfer (SANS)

M. Schaal, P. Lamparter, and S. Steeb

Max-Planck-Institut für Metallforschung, Institut für Werkstoffwissenschaften, Stuttgart

Z. Naturforsch. **43a**, 1061–1064 (1988); received September 17, 1988

By means of small angle neutron scattering SANS using isotopic substitution the medium range structure of the amorphous $Ni_{63}Nb_{37}$-alloy was investigated. From the coherently scattered intensity in the region of small momentum transfer the total and partial Bhatia-Thornton structure factors were determined. For Q-values down to 0.03 $Å^{-1}$ no small angle scattering effect at all was observed. Compared to amorphous $Ni_{80}P_{20}$ this means that apparently no small regions exits in amorphous $Ni_{63}Nb_{37}$. For $0.008\ Å^{-1} \leq Q \leq 0.03\ Å^{-1}$, corresponding to correlation lengths between 800 and 200 Å, however, S_{CC} and S_{NN} increase with almost constant slope of about 3.6 in the log $S(Q)$ − log Q presentation.

1. Introduction

Metal-metalloid glasses are not homogeneous, as was shown with $Fe_{80}B_{20}$ [1], $Ni_{81}B_{19}$ [2], and $Ni_{80}P_{20}$ [3] by means of small angle scattering technique. To contribute to the question whether metal-metal glasses are more homogeneous, the neutron scattering behaviour of amorphous $Ni_{63}Nb_{37}$ at small momentum transfer (SANS) was studied, and furthermore the method of isotopic substitution was used in order to evaluate the three partial Bhatia-Thornton structure factors S_{NN}, S_{CC}, and S_{NC}. These represent the description of the structure in terms of density- and concentration-fluctuations [4]. The short range order structure of amorphous Ni-Nb-alloys has been studied in the region of large momentum transfer using neutrons [5, 6] and X-rays [7], respectively.

2. Theoretical Fundamentals

The total Bhatia-Thornton [4] structure factor $S^{BT}_{tot}(Q)$ is obtained from the coherently scattered intensity per atom $I_{coh}(Q)$:

$$S^{BT}_{tot}(Q) = I_{coh}(Q)/\langle b^2\rangle \tag{1}$$

with

$\langle b^2\rangle = c_1 b_1^2 + c_2 b_2^2$,

b_1, b_2 = coherent scattering length of component 1, 2,

c_1, c_2 = atomic fraction of component 1, 2,

$Q = 4\pi(\sin\Theta)/\lambda$, 2Θ = scattering angle,

λ = wavelength.

The total structure factor can be presented as sum of the contributions of the three Bhatia-Thornton partial structure factors as follows [4]:

$$S^{BT}_{tot}(Q) = \frac{\langle b\rangle^2}{\langle b^2\rangle} S_{NN}(Q) + \frac{c_1 c_2 (\Delta b)^2}{\langle b^2\rangle} S_{CC}(Q) + \frac{2\langle b\rangle \Delta b}{\langle b^2\rangle} S_{NC}(Q) \tag{2}$$

with

$$\Delta b = b_1 - b_2, \quad \langle b\rangle = c_1 b_1 + c_2 b_2,$$

$S_{NN}(Q)$ = contribution of the correlations between density-fluctuations,

$S_{CC}(Q)$ = contribution of the correlations between concentration-fluctuations,

$S_{NC}(Q)$ = contribution of the correlations between density- and concentration-fluctuations.

$S_{NN}(Q)$ is determined by the topological arrangement of the atoms, i.e. by the local number density. $S_{CC}(Q)$ is determined by the distribution of the different

Reprint requests to Prof. Dr. S. Steeb, Max-Planck-Institut für Metallforschung, Institut für Werkstoffwissenschaften, Seestraße 92, D-7000 Stuttgart 1

0932-0784 / 88 / 1200-1061 $ 01.30/0. – Please order a reprint rather than making your own copy.

atomic species. For different atomic sizes, however, the additional contribution $S_{NC}(Q)$ to the total structure factor occurs.

3. Experimental

For the structural investigation of $Ni_{63}Nb_{37}$ the isotopic substitution method was applied using the isotopes as compiled in Table 1. Since ^{62}Ni shows a negative scattering length, a zero scattering mixture $^{\phi}Ni$ can be produced from ^{60}Ni and ^{62}Ni. Table 1 also contains the corresponding cross sections for scattering σ^s and absorption σ^a.

The three investigated specimens were $^{nat}Ni_{63}Nb_{37}$, $^{62}Ni_{63}Nb_{37}$, and $^{\phi}Ni_{63}Nb_{37}$, for which the weighting factors corresponding to (2) are given in the equations:

$$^{nat}Ni_{63}Nb_{37}: \; ^{nat}S(Q) = 0.971\, S_{NN}(Q) + 0.029\, S_{CC}(Q) + 0.693\, S_{NC}(Q), \quad (3)$$

$$^{62}Ni_{63}Nb_{37}: \; ^{62}S(Q) = 0.116\, S_{NN}(Q) + 0.884\, S_{CC}(Q) + 1.326\, S_{NC}(Q), \quad (4)$$

$$^{\phi}Ni_{63}Nb_{37}: \; ^{\phi}S(Q) = 0.370\, S_{NN}(Q) + 0.630\, S_{CC}(Q) - 2.000\, S_{NC}(Q). \quad (5)$$

From the large differences between the coefficients in this system of three linear equations follows that the three partials can be very well determined. The normalized coefficient-determinant, whose possible maximum value can be unity, amounts to 0.661.

The specimens were produced with the melt-spin procedure and then investigated with the D17 instrument at ILL, Grenoble [9], using $\lambda = 12$ Å. The sample-detector distance amounted to 3.3 m. The two dimensional intensity distribution recorded with the area detector was converted to a one dimensional distribution (see Figure 1). Thereby the intensity scattered within two opposite sectors, each 67.5° wide parallel to the ribbon direction, was integrated. Then the experimental data in the log-log presentation were smoothed using a polynom fit.

Table 1. Absorption- and scattering data [8]. $\sigma^s = \sigma^{coh} + \sigma^{incoh.}$, $\sigma^{coh} = 4\pi b^2$. The σ^a are given for $\lambda = 12$ Å.

Element; isotope	b [10^{-12} cm]	σ^s [barn]	σ^a [barn]
^{nat}Ni	1.03	17.56	30
^{60}Ni	0.28	0.96	19.3
^{62}Ni	−0.87	9.6	96.7
$^{\phi}Ni = {}^{60}Ni_{75.65}{}^{62}Ni_{24.35}$	0.0	3.051	38
Nb	0.7054	6.25	7.7

The experimental intensity data were corrected for background as well as absorption and then normalized to absolute units by comparison with the incoherent scattering from a vanadium standard.

4. Results and Discussion

Figure 1 shows the log-log plot of $S_{tot}(Q)$ versus Q. It should be noted that the Guinier plot [10], i.e. $\ln S_{tot}(Q)$ vs Q^2, yielded no straight line, thus indicating that no regions with one defined radius exist.

For $\log Q \leq -1.7$ the plots for all three specimens in Fig. 1 show a nearly parallel run. $^{nat}Ni_{63}Nb_{37}$ yields a rather linear run, as has been observed frequently in the case of metallic glasses [1–3]. Conclusions concerning the magnitude of the partials can already be drawn regarding Fig. 1 together with (3), (4) and (5). In Fig. 1 the $^{nat}Ni_{63}Nb_{37}$-specimen yields the lowest structure factor. According to the equations this can only be understood if the scattering is dominated by $S_{CC}(Q)$, which for the case of $^{nat}Ni_{63}Nb_{37}$ enters with a small weighting factor.

However, Fig. 1 shows clearly that apparently the interpretation of total structure factors is not conclusive since the three plots obtained from one and the same amorphous system differ appreciably. A real insight into the medium range structure can only be obtained regarding the partial structure factors which

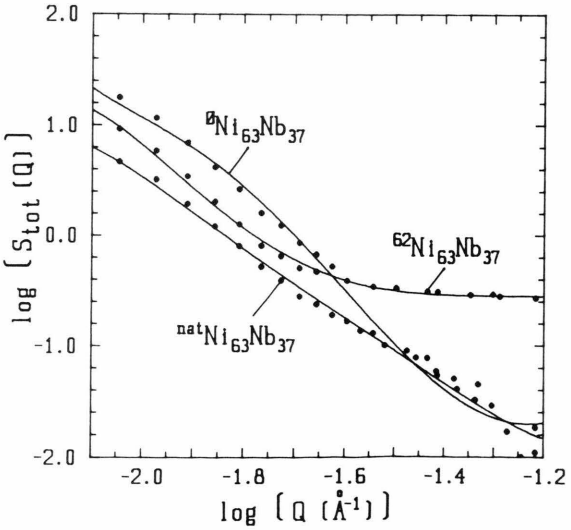

Fig. 1. Neutron diffraction; log $S(Q)$ versus log Q for the amorphous specimens $^{nat}Ni_{63}Nb_{37}$, $^{62}Ni_{63}Nb_{37}$, $^{\phi}Ni_{63}Nb_{37}$. • experimental data, —— smoothed.

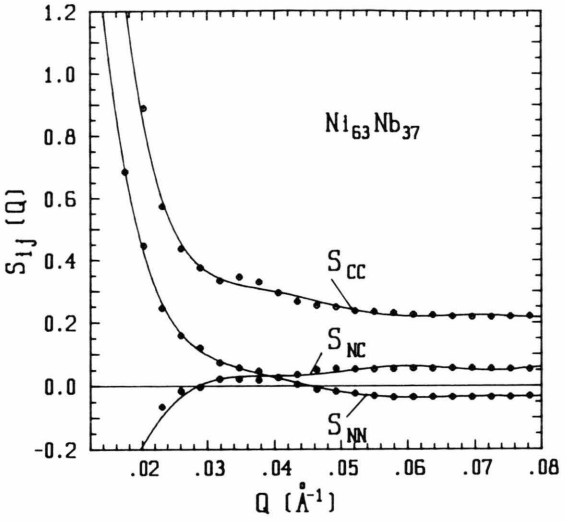

Fig. 2. Amorphous $Ni_{63}Nb_{37}$; Bhatia-Thornton partial structure factors at larger Q's.

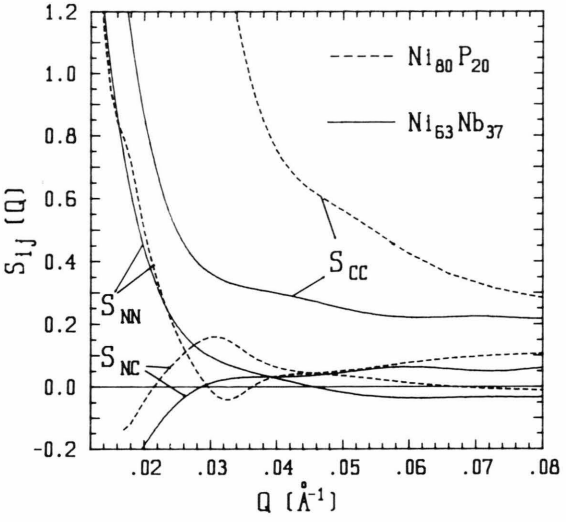

Fig. 4. Amorphous $Ni_{63}Nb_{37}$ (——) and $Ni_{80}P_{20}$ (– – –); Bhatia-Thornton partial structure factors at larger Q's.

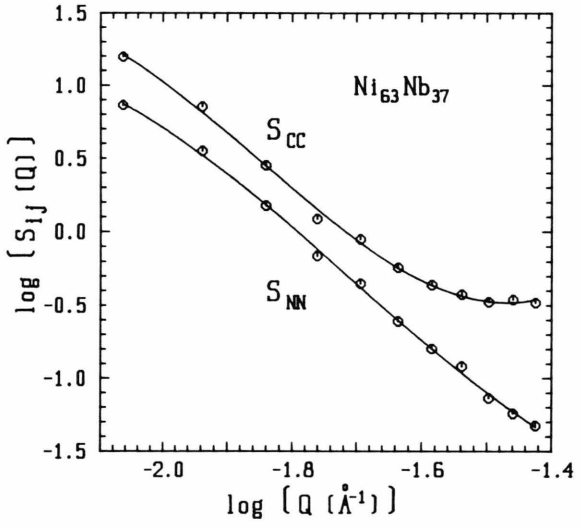

Fig. 3. Amorphous $Ni_{63}Nb_{37}$; Bhatia-Thornton partial structure factors S_{CC} and S_{NC} at smaller Q's.

are physically relevant because they are independent of the special experimental conditions, i.e. of the scattering lengths.

In Fig. 2 we present for amorphous $Ni_{63}Nb_{37}$ the three partial Bhatia-Thornton structure factors as obtained from the totals of Fig. 1 using the Eqs. (3), (4), and (5) in the Q-region $0.01\,\text{Å}^{-1} \leq Q \leq 0.08\,\text{Å}^{-1}$. For the smaller Q-values $0.008\,\text{Å}^{-1} \leq Q \leq 0.04\,\text{Å}^{-1}$ we show in Fig. 3 $\log S_{CC}(Q)$ and $\log S_{NN}(Q)$ vs. $\log Q$.

For the further discussion of the partial functions we present them in Figs. 4 and 5 once more together with those obtained with amorphous $Ni_{80}P_{20}$ [3].

According to Fig. 4 $S_{NN}(Q)$ and $S_{NC}(Q)$ as obtained with amorphous $Ni_{63}Nb_{37}$ and amorphous $Ni_{80}P_{20}$ show down to $Q = 0.03\,\text{Å}^{-1}$ no small angle scattering effect.

For the case of $Ni_{63}Nb_{37}$ the $S_{CC}(Q)$-function does not show a small angle scattering for $Q > 0.04\,\text{Å}^{-1}$. This is in contrast to the metal-metalloid-glass $Ni_{80}P_{20}$, where the small angle scattering of $S_{CC}(Q)$ for $Q > 0.04\,\text{Å}^{-1}$ could be attributed to so called "small regions" with diameters of about 15 Å. Apparently in the metal-metal glass $Ni_{63}Nb_{37}$ no small regions exist.

Concerning smaller Q's we regard Fig. 5 and state that the levels of $S_{CC}(Q)$ and $S_{NN}(Q)$ are not very different for amorphous $Ni_{63}Nb_{37}$ whereas in the case of amorphous $Ni_{80}P_{20}$ $S_{CC}(Q)$ was appreciably larger than $S_{NN}(Q)$. The two $Ni_{63}Nb_{37}$-curves show almost the same slope of about -3.6. Whether this linear slope continues to smaller Q's must be investigated by further experiments. If so, this would correspond to a scattering from fractional inner surfaces with fractal surface dimension $D_S = 2.4$. One possible explanation for this behaviour would be the following: Amorphous $Ni_{63}Nb_{37}$ consists of a matrix containing regions which differ in their concentration from the matrix and which are separated from the matrix by the inner surfaces mentioned above.

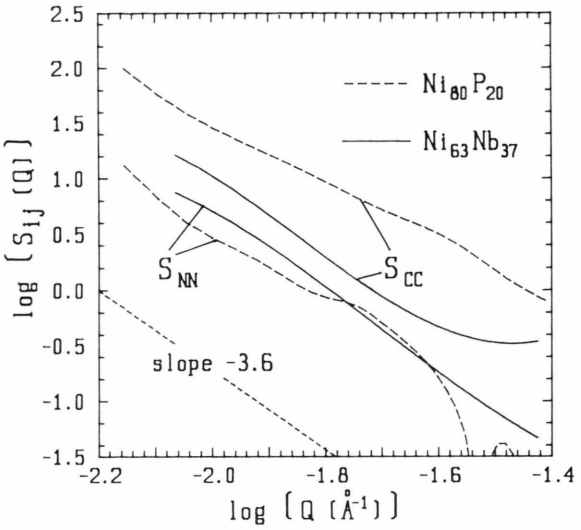

Fig. 5. Amorphous $Ni_{63}Nb_{37}$ (——) and $Ni_{80}P_{20}$ (– – –); Bhatia-Thornton partial structure factors S_{CC} and S_{NC} at smaller Q's.

Taking the level of $S_{CC}(Q)$ as a measure for the inhomogeneity of an amorphous substance we can conclude from Fig. 5 that the metal-metal glass $Ni_{63}Nb_{37}$ is more homogeneous than the metal-metalloid glass $Ni_{80}P_{20}$. With respect to this finding we refer to a FIM study on $Ni_{61}Nb_{39}$ [11], where in contrast to metal-metalloid glasses [12] no evidence for compositional inhomogeneities has been reported.

In connection to the behaviour of amorphous $Ni_{63}Nb_{37}$ at very small Q's we refer to [13], where amorphous $Ni_{32}Pd_{52}P_{16}$ was studied down to $Q = 8 \cdot 10^{-4}$ Å^{-1} with surface fractal dimensions D_S in the region $2.15 \leq D_S \leq 2.77$ depending on the annealing conditions.

Acknowledgements

Thanks are due to Deutsche Forschungsgemeinschaft, Bad Godesberg for financial support of this work and to ILL for allocation of beam time.

[1] E. Nold, S. Steeb, and P. Lamparter, Z. Naturforsch. **35a,** 610 (1980).
[2] K. Schild, P. Lamparter, and S. Steeb, "Current Topics on Non-Crystalline Solids", ed. M. D. Baró, N. Clavaguera, World Scientific, 253 (1986).
[3] K. Schild, F. Frisius, P. Lamparter, and S. Steeb, Z. Naturforsch. **40a,** 551 (1985).
[4] A. Bhatia and D. E. Thornton, Phys. Rev. **B2,** 3004 (1970).
[5] E. Sváb, L. Köszegi, G. Mészáros, J. Takács, S. N. Ishmaev, S. L. Isakov, I. P. Sadikov, and Chernyshov, **LAM6,** 5 (1985).
[6] P. Lamparter, M. Schaal, and S. Steeb, ILL Reports and Theory College Activities **1986,** 232
[7] H. S. Chen and Y. Waseda, Phys. Stat. Sol. (a) **51,** 593 (1979).
[8] L. Koester and W. B. Yelon, Neutron Diffraction Newsletter 1983.
[9] Neutron Research Facilities at the ILL High Flux Reactor, Edition 1986; Institut-Max von Laue-Paul Langevin, Grenoble, Frankreich 1986, p. 59.
[10] H. Guinier and G. Fournet, Small Angle Scattering of X-Rays, John Wiley & Sons Inc., London 1955.
[11] R. Grüne, M. Gehring, R. Wagner, and P. Haasen, Proc. RQ5, 761 (1985).
[12] J. Piller and P. Haasen, Acta Met. **30,** 1 (1982).
[13] M. Schaal, P. Lamparter, and S. Steeb, Z. Naturforsch. **43a,** 1055 (1988).